PHYSICAL REVIEW B **69**, 085213 (2004)

Energetics and diffusivity of indium-related defects in silicon

Paola Alippi,* Antonino La Magna, Silvia Scalese, and Vittorio Privitera
CNR-IMM, Sezione Catania, Stradale Primosole 50, I-95121 Catania, Italy
(Received 12 September 2003; revised manuscript received 5 November 2003; published 27 February 2004)

We present a theoretical investigation on In-related defects in silicon, aimed at understanding In interactions with native defects, vacancy (V) and self-interstitial (I), and at determining the energy parameters needed to efficiently simulate and interpret the experimental profiles. *Ab initio* total-energy calculations within density-functional theory and in the generalized gradient approximation are performed in order to investigate equilibrium geometries and formation energies of substitutional In, In-I, and In-V complexes. We determine the migration energies of I- and V-mediated diffusion mechanisms, discussing the location of saddle points along the minimum-energy paths. Moreover, we report anomalous characteristics of the interactions between In and V with respect to other *p*-like dopants. The *ab initio* energetics are then implemented into a continuum model for In diffusion. This allows the accurate simulations of experimental secondary-ion-mass-spectroscopy profiles of implanted and annealed samples, at various process conditions (i.e., annealing temperature, implant energy).

DOI: 10.1103/PhysRevB.69.085213 PACS number(s): 61.72.Tt, 71.15.Mb, 66.30.Jt, 61.72.Ss

I. INTRODUCTION

Heavy-ion implantation is one of the promising methods for achieving very shallow junctions in microelectronic devices. Due to its heavier mass, indium could be an alternative to boron as *p*-dopant in silicon, in order to realize shallower and steeper profiles required by ultra-large-scale integration technology.[1,2] However, the main drawback of In doping is the poor electrical activation due to high ionization energy.[3,4] Furthermore, a strong tendency of In to out diffuse from Si wafers during thermal processes and a low solid solubility have been observed.[4] These phenomena determine a further limitation to the maximum fraction of In atoms that can be electrically activated. A possible way to increase the low activation is to promote the formation of In-impurities complexes, which shifts down the electronic level towards the valence-band edge. Recent experimental works[3–5] have shown that when C atoms are present, either as impurities or as coimplanted species, the In-C complex can form and a shallower In-related acceptor level appears.[6]

Diffusion of In in silicon has been investigated in several experimental works, observing enhanced anomalous effects whenever a supersaturation of interstitial silicon atoms is present.[1,2,4,7] In order to extract indium diffusion parameters, process simulators have been usually adopted,[1,2,4] modeling diffused In profiles in ion-implanted samples or in oxidizing conditions. In this way, a diffusion mechanism via silicon self-interstitial atoms has been proposed as dominant over that mediated by silicon vacancies,[2,7] while an estimation of the activation energy $E_{act} \simeq 3.6$ eV in intrinsic conditions has been given by Suzuki *et al.*[8]

Due to the lack of atomistic theoretical investigations on In interactions with silicon defects, process simulators have obviously had to rely on well educated guesses on In behavior in silicon, argued from the successful fitting of the experimental data and from the analogies with other dopants behavior, such as boron. However, it is clear that any similarity should be critically considered, in view of the different atomic radii of the two species. For instance, simple arguments based on the lattice strain induced by the dopant in the host matrix would favor the formation of B-interstitial complexes over B-vacancy ones, while the opposite argument should be valid for indium.

We present a theoretical investigation on In defects in silicon, aimed at providing a well-founded *ab initio* picture of defect energetics and diffusivity over which a continuum diffusion model is then built. The hierarchical method we have adopted is not only meant to efficiently simulate the available experimental profiles, but, more generally, to give a microscopic insight on indium-silicon interactions. From a first-principle study of In interactions with native defects in silicon, we obtain in fact the energetics of different complexes formed by In with vacancies and self-interstitials together with the diffusion parameters. We then integrate the *ab initio* results into a continuum model that allows a direct comparison with experimental data. The diffused profiles obtained by our modeling are in fact compared to those measured by secondary-ion-mass spectroscopy (SIMS) after implantation and thermal annealing, showing a noteworthy agreement.

The paper is organized as follows. The *ab initio* results are reported in Sec. II. After a brief description (Sec. II A) of the computational framework, the results for substitutional In and a discussion on In solid solubility limit are presented (Sec. II B). We turn then to the investigation of In interactions with silicon native defects: Secs. II C and II D report the energetics, diffusion mechanisms, and migration barriers of In complexes with interstitials and vacancies, respectively. The implementation of the *ab initio* investigations into a continuum model for In diffusion is presented in Sec. III, where the results of the diffusion simulations are also compared to the SIMS profiles.

II. *Ab initio* RESULTS

A. Computational framework

The *ab initio* calculations are performed within density-functional theory (DFT) and using the Vienna *ab initio* simu-

 ©2004 The American Physical Society

lation package (VASP).[9] We perform our calculations within the generalized gradient approximation (GGA), in the Perdew-Wang formulation.[10]

In general, we calculate the formation energy E_f of q-charged defects (def^q) from $E(\mathrm{def}^q)$, the total energy of the supercell containing N_{Si} Si atoms and N_{In} In atoms, as

$$E_f(\mathrm{def}^q)=E(\mathrm{def}^q)-N_{\mathrm{Si}}\mu_{\mathrm{Si}}-N_{\mathrm{In}}\mu_{\mathrm{In}}+q\mu_F, \qquad (1)$$

where μ_F is the electron chemical potential (the Fermi level), and μ_{Si}, μ_{In} are the chemical potentials of the host and dopant atomic species, respectively. In the following, the chemical potential of Si atoms, μ_{Si}, is always chosen as the cohesive energy of bulk silicon, $\mu_{\mathrm{Si}}(bulk)$. As will be discussed in the following, we set the In chemical potential at the bulk energy of crystalline In $[\mu_{\mathrm{In}}(bulk)]$ when we calculate the formation energy of substitutional In (In_s^q) and determine the value of In solid solubility in silicon. However, since we are then interested in discussing the formation of In-I and In-V (in general, In-X^q) complexes after implantation and thermal annealing processes, a different choice of μ_{In} is made in Secs. II C and II D. In these cases, in fact, it is natural to consider a reservoir of substitutional atoms for the dopant species. Therefore, we fix the value of μ_{In} by setting the formation energy of In_s^0 as the reference energy for all In-X^q defects.

We consider also formation energy differences between initial and final products of reactions involving a In-X complex and isolated I, V, In_s defects, i.e., of the form $\mathrm{In}_s^{q_1}+X^{q_2}\rightarrow\mathrm{In}\text{-}X^{q_1+q_2}$. In the following, we define for each In-X^q the binding energy $E_b(\mathrm{In}\text{-}X^q)$ as the smallest formation energy difference among all possible dissociation reactions.

In order to converge all properties of relevance, we use a cutoff energy $E_c=207$ eV for the plane-wave expansion and a Monkhorst-Pack $(4\times4\times4)$ grid for the **k**-space summation. Ultrasoft pseudopotentials[11] describe the electron-ion interactions. The In pseudopotentials include the semicore $4d$ electrons in the valence. The supercell unit cell that is periodically repeated in space contains 64 atoms. We test that the calculated formation energy values of neutral defects differ by less than 50 meV when the cutoff energy is raised to 285 eV, the **k**-point sampling set is set to $(5\times5\times5)$, or a larger simulation cell is chosen. For charged defects, a uniform jellium background of opposite charge maintains the charge neutrality of the simulation cell, and the total energy $E(\mathrm{In}\text{-}X^q)$ in Eq. (1) is corrected by taking into account monopole-monopole and monopole-quadrupole terms.[12] We test that total-energy corrections induced by neglecting quadrupole-quadrupole terms are smaller than 50 meV.

B. Substitutional In

The presence of substitutional In in the Si host matrix induces outward relaxations of the nearby silicon atoms, as is expected from the larger atomic radius of In with respect to Si. The calculated In-Si first-neighbor distances of the relaxed In_s^0 structure are in fact $\simeq 7\%$ larger than $d_{\mathrm{Si}}=2.36$ Å, the calculated GGA atom spacing in bulk silicon. From Eq. (1) and taking for μ_{In} the DFT-GGA value of the cohesive energy of body-centered In calculated by Zoroddu *et al.*,[13] we calculate the formation energy of neutral substitutional In, $E_f(\mathrm{In}_s^0)=1.46$ eV.

The atomic relaxations around the negatively charged substitutional In (In_s^-) do not appreciably differ from those of the neutral In_s. Since the ionization level $\epsilon(q/q')$ is defined as the value of μ_F at which the q'-charged defect becomes energetically favorable over the q-charged one [i.e., where $E_f(\mathrm{def}^{q'})=E_f(\mathrm{def}^q)$], we obtain $\epsilon(0/-)=187$ meV. We mention that all values of the electron energy levels are referred here to the valence-band maximum. This value is in very good agreement with the experimental acceptor level associated with In_s, $\epsilon(0/-)=156$ meV.[14] As mentioned in Sec. II A this discrepancy is of the order of the computational confidence on formation energies ($\simeq 50$ meV).

In order to discuss In solid solubility, we first calculate N_{In}, the maximum concentration of isolated neutral In impurities in the silicon matrix at a given temperature T, and in conditions of thermodynamic equilibrium. This quantity is obtained from the formation energy $E_f(\mathrm{In}_s^0)$ and the density of atomic sites in bulk Si, ρ_{Si}, as $N_{\mathrm{In}}=\rho_{\mathrm{Si}}\exp[-E_f(\mathrm{In}_s^0)/k_BT]$. The calculated values of N_{In} range from $0.71\times10^{11}\ \mathrm{cm}^{-3}$ at $T=30\,^\circ\mathrm{C}$ to $0.13\times10^{16}\ \mathrm{cm}^{-3}$ at $T=700\,^\circ\mathrm{C}$, and $0.81\times10^{17}\ \mathrm{cm}^{-3}$ at $T=1000\,^\circ\mathrm{C}$.

As discussed above, the range of possible applications of In doping in microelectronic devices is partially limited by its high ionization energy and by the relatively low values of solid solubility, i.e., the low density of In atoms in the electrically active substitutional configuration. To this respect, we turn to the calculation of the density of ionized In atoms, N_{In}^-, as a function of the temperature T, using the following equation:[15]

$$N_{\mathrm{In}}^-(T)=\frac{N_{\mathrm{In}}}{1+4\exp\{[\epsilon(0/-)-\mu_F]/k_BT\}}. \qquad (2)$$

The charge neutrality condition sets the value of the Fermi level μ_F in Eq. (2), equating the positive hole density in the valence band to the sum of the electron density in the conduction band and the concentration of negatively charged In_s^- ions, i.e.,

$$N_V\exp\left(-\frac{\mu_F}{k_BT}\right)=N_C\exp\left(-\frac{E_g-\mu_F}{k_BT}\right)+N_{\mathrm{In}}^-. \qquad (3)$$

Here, N_C and N_V are the electron and hole density at the conduction- and valence-band edges, respectively, and E_g is the band gap. We can solve for μ_F from the expressions above and calculate the fraction of ionized acceptors $N_{\mathrm{In}}^-(T)$. In doing this, we first use[16] in Eq. (2) the value of N_{In} calculated at $T_g=1000\ ^\circ\mathrm{C}$ to distinguish the temperature T at which electrical activity is measured from that at which In atoms are introduced in the sample as, for instance, by solid phase diffusion. In this way, we obtain values of the ionized atom concentration ranging from $N_{\mathrm{In}}^-=0.13\times10^{17}\ \mathrm{cm}^{-3}$ at room temperature to $N_{\mathrm{In}}^-=0.71\times10^{17}\ \mathrm{cm}^{-3}$ at $T=300\,^\circ\mathrm{C}$

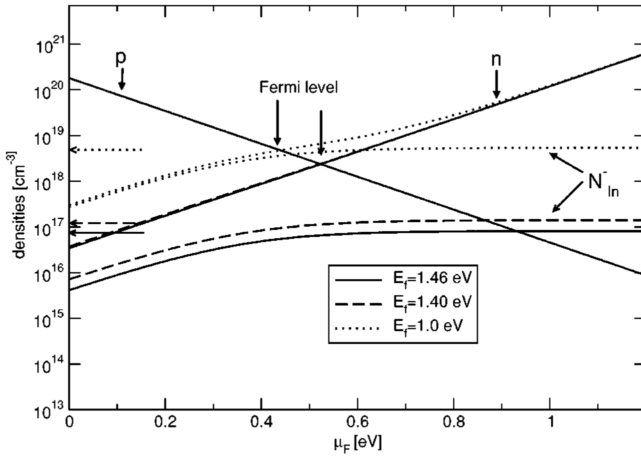

FIG. 1. Total positive (p), negative (n), and ionized acceptor densities (N_{In}^{-}) as functions of the Fermi energy μ_F, at $T = 1100\,°\mathrm{C}$. $N_{\mathrm{In}}^{-}(\mu_F)$, $p(\mu_F)$, and $n(\mu_F)$ are plotted with same style (solid, dashed, and dotted lines), each corresponding to different values of E_f (1.46 eV, 1.40 eV, 1.0 eV), as indicated in the legend. The horizontal arrows point to the acceptor densities corresponding to the self-consistent value of μ_F, also indicated by vertical arrows.

and $N_{\mathrm{In}}^{-} = 0.76\times 10^{17}\ \mathrm{cm}^{-3}$ at $T = 1000\,°\mathrm{C}$, corresponding to 16%, 87%, and 91% of the ion concentration $N_{\mathrm{In}}(T_g)$.

Experimentally, the highest value of solid solubility has been obtained after ion implantation and thermal annealing by Solmi *et al.*[4] From the measured values of hole concentration and estimating that $\simeq 15\%$ of In is electrically active at room temperature, they conclude that In solubility is $\simeq 1.8\times 10^{18}\ \mathrm{cm}^{-3}$, for annealing temperatures T in the range 700–1100 °C. In these experimental conditions, dopants are introduced by ion implantation, and thermal annealing processes are then used to relax the lattice damage. Thus, the concentration of substitutional In available to be electrically activated might not be equivalent to that obtained when the doping is achieved by solid phase diffusion at thermal equilibrium, $N_{\mathrm{In}}(T_g)$. In particular, the comparison with the calculated values reported above should be critically considered if the peak concentration of the implanted dose is lower than $N_{\mathrm{In}}(T_g)$. However, this is not the case in the experiments of Solmi *et al.*[4] and we observe that our theoretical findings are in good agreement with the experimental limiting value.

Given the exponential dependence of N_{In}^{-} on E_f, we discuss the accuracy of our calculated values of ionized dopant concentrations. In Fig. 1, we plot the ionized In concentrations $N_{\mathrm{In}}^{-}(\mu_F)$ together with the total positive hole density $p(\mu_F)$ and the negative electron density $n(\mu_F)$, as calculated from Eqs. (2) and (3) at $T = 1100\,°\mathrm{C}$. This is a graphical way of solving the above equations, since the crossing of $p(\mu_F)$ and $n(\mu_F)$ [the left- and right-hand sides of Eq. (3)] determines the Fermi energy of the system. The latter then sets the calculated active dopant concentration N_{In}^{-}, indicated with horizontal arrows in the picture. We plot with solid lines the curves obtained inserting the DFT-GGA values of formation energy and acceptor level [$E_f = 1.46$ eV, $\epsilon(0/-) = 187$ meV, solid lines], while the dashed lines correspond to values differing by the typical computational error, i.e., $\Delta \simeq 50$ meV. As is evident from Fig. 1, the self-consistent value of the Fermi energy does not change dramatically for these variations in E_f and the estimation of the active dopant concentration varies by less than one order of magnitude.

The formation energy, and hence the solubility, is also determined by the chemical potential μ_{In}. In thermodynamic equilibrium, the latter equals $\mu_{\mathrm{In}}(bulk)$. A larger (less negative) value of μ_{In}, obtained, e.g., by means of nonequilibrium growth processes, would of course enhance the solubility. This could be the case if a reservoir of dopant atoms could be stabilized at the surface by carefully tailoring the experimental conditions. *Ab initio* calculations of absorption energies of B atoms on different sites of Si surfaces[16] have indeed shown that this is the case: initial incorporation of B at the growing surface costs more energy than having the dopant in its bulk form. The highest value of μ_{B} under epitaxial conditions corresponds to spontaneous accumulation of B at the top surface layer, i.e., when surface adsorption energy $E_{ad}(\mu_{\mathrm{B}}^{\mathrm{surf}}) = 0$. This condition would set a higher B chemical potential with respect to $\mu_{\mathrm{B}}(bulk)$, by $\simeq 0.5$ eV, and a corresponding smaller formation energy for B_s.

As regards indium, the *ab initio* work of Northrup and co-workers[17] found that the stable In:Si(001) structure is a 2×2 ad-dimer, oriented parallel to the Si-Si surface dimer, with surface adsorption energy $E_{ad}(\mu_{\mathrm{In}})$ lower than that of any other geometry considered there, for any choice of μ_{In}. From their $E_{ad}(\mu_{\mathrm{In}})$ values we extrapolate $\mu_{\mathrm{In}}^{\mathrm{surf}} \simeq \mu_{\mathrm{In}}(bulk) + 1.0$ eV. Such variation of μ would indeed affect $\mathrm{In_s}$ formation energy and thus In solubility in the same direction as for B. In fact, in Fig. 1, a sizable increase of N_{In}^{-} and a decrease of the Fermi level can be noted if a smaller E_f is used in Eq. (2) ($E_f[\mathrm{In_s^0}] = 1.0$ eV, dotted lines).

These effects, much larger than those due to typical computational accuracy, would indicate that, if the incorporation of In at the Si surface causes an increase of the chemical potential, the active In concentration is affected in a sizable way. This could be the case, for instance, in molecular-beam epitaxial growth. Although this is a qualitative argument and VASP calculations of E_{ad} would be needed for a consistent comparison, we suggest that exploring experimental conditions that set different atomic reservoirs than the bulk dopant phase might be a possible efficient way to increase In solubility in silicon.

C. In-interstitial defects

Among all neutral In-related defect configurations containing an interstitial atom, the lowest-energy structure consists of a $\mathrm{In_s}$ atom with a Si interstitial in a nearby tetrahedral (Td) position, shown in Fig. 2(a) and denoted in the following as InI. The defect has C_{1h} symmetry and formation energy $E_f = 2.6$ eV. This value is calculated from Eq. (1), taking the formation energy of $\mathrm{In_s^0}$ as reference energy. In the relaxed configuration, nearest-neighbor (nn) In-Si distances are larger than d_{Si}. Starting from the initial guessed geometry, with the atoms placed in the ideal substitutional and tetrahedral positions of the silicon lattice, the relaxation af-

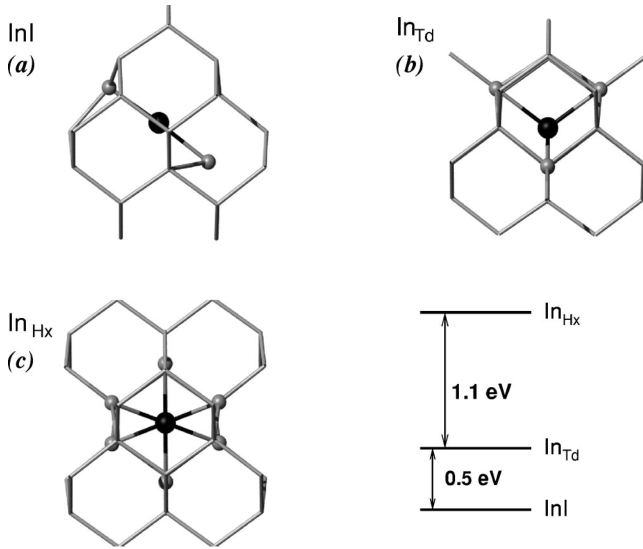

FIG. 2. Relaxed DFT configurations of neutral interstitial In defects, InI, In_{Td}, and In_{Hx} (see text). The atoms that have undergone sizable relaxations from the initial structure are shown with spheres over the host silicon lattice (sticks). The In atom is shown as a black sphere, its nearest-neighbor Si atoms with smaller gray spheres. On the right-hand side (bottom), the formation energy differences among the three structures are reported.

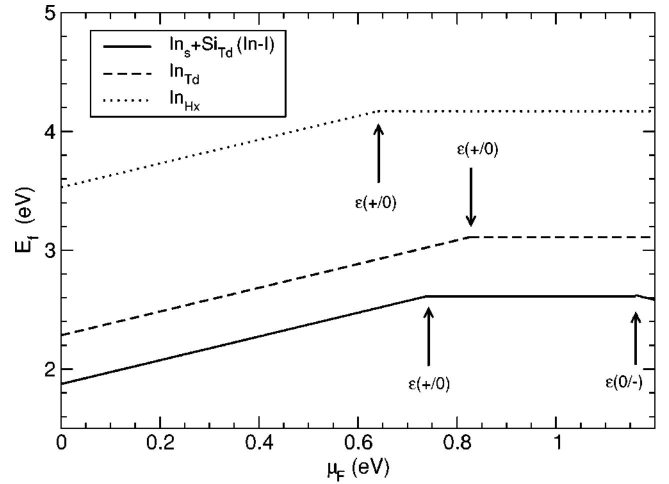

FIG. 3. Formation energies of In-interstitial defects, InI, In_{Td}, and In_{Hx} as functions of the Fermi level μ_F. The electronic levels ϵ are also indicated.

fects mainly the atomic position of In_s and of its two nn atoms, i.e., Si_{Td} and the Si atom that lies on the same $\langle 111\rangle$ direction of the In-Si_{Td} bond, opposite to Si_{Td}. In particular, these two In-Si bonds result to be $\simeq 7\%$ longer than d_{Si}. The other Si atoms hardly move from their ideal lattice sites, making weaker bonds to In, with $d_{In\text{-}Si} \simeq 2.7$ Å. Considering the formation reaction $In_s^- + I^+ \rightarrow InI^0$ and using the GGA value of the formation energy of the dumbbell Si interstitial,[18] we calculate $E_b(InI^0) = -1.2$ eV.

The configurations with In sitting in interstitial sites, the tetrahedral In_{Td}, and the hexagonal defect In_{Hx} [Figs. 2(b,c)] have larger formation energy with respect to InI. In both cases, the relaxed In-Si bonds are larger than the distances of the ideal Td and Hx sites from the neighboring lattice sites. Placing an interstitial In in a Td or Hx site induces large outward atomic relaxations of *all* its nn Si atoms. This radial strain relaxation affects also the Si atoms in the next nn shell, inducing a $\simeq 10\%$ increase of Si-Si distances. On the other hand, in the InI configuration, only the first nn's of In are involved in the strain relaxation, which extends along the $\langle 111\rangle$ direction.

A third interstitial structure, with In in a bond-centered (BC) position between two silicon atoms, is unstable and relaxes towards the InI geometry. The same behavior is observed for the mixed In-Si $\langle 110\rangle$- and $\langle 100\rangle$-dumbbell configurations.

The InI configuration is the lowest-energy one for all values of Fermi level μ_F, as is evident from Fig. 3, where we plot $E_f(\text{In-}I^q;\mu_F)$, i.e., the formation energy as a function of μ_F for the In-interstitial defects in the charge states 0, $+$, and $-$. Atomic relaxations do not change substantially between neutral and charged defect configurations. Figure 3 shows that all interstitial-related defects are donors in the p-type to intrinsic conditions, i.e., for $\mu_F \leqslant E_g/2$. The levels are $\epsilon(+/0)[\text{InI}] = 0.74$ eV, $\epsilon(+/0)[\text{In}_{Td}] = 0.83$ eV, and $\epsilon(+/0)[\text{In}_{Hx}] = 0.68$ eV. On the other hand, all $\epsilon(0/-)$ ionization levels of the In-interstitial defects fall inside the conduction band (with $\epsilon(0/-)[\text{InI}] = 1.16$ eV).

In order to determine the activation energy for the interstitial-mediated diffusion process, it is necessary to identify the migration path of the InI complex and to locate the saddle point. This is usually done with the aid of computational techniques that are capable of searching the minimum-energy path in the defect configurations space, as the nudged elastic band[19] (NEB) method, implemented in VASP. Nevertheless, it is possible to estimate the activation energy of I-mediated diffusion from our calculated energetics. We consider two possible migration paths for the neutral defect. The first one is the so-called *interstitialcy* mechanism, which also characterizes the diffusion of boron in conditions of interstitial supersaturation:[20] starting from the ground-state configuration [Fig. 2(a)], the dopant is kicked out into an interstitial position, while Si_{Td} goes to the lattice site. Indium then falls into a different nearby substitutional position, kicking out a Si atom in a Td position and forming a new InI complex. Along the path, the increase in energy cannot exceed the ground-state binding energy $E_b(\text{InI}) = -1.2$ eV, otherwise the defect might dissociate before the diffusion step is completed. This excludes the hexagonal site as a saddle point, since $E_b(\text{Hx}) = +0.4$ eV, and points out to the In_{Td} configuration. Since $E_f(\text{In}_{Td}) - E_f(\text{InI}) = 0.5$ eV, the minimum migration energy is 0.5 eV$\leqslant E_m \leqslant 1.2$ eV, hence the activation energy, $E_{act} = E_f + E_m$, would result to be 3.1 eV$\leqslant E_{act} \leqslant 3.8$ eV.

A different path connects two InI configurations centered on different lattice sites, with the BC position as the saddle point. Through a constrained calculation of the energy of the BC configuration, we find a small-energy barrier ($\simeq 0.3$ eV) from InI to In-BC. In this way, however, In moves only between two adjacent lattice sites, lying on the same $\langle 111\rangle$ direction of the initial In-Si_{Td} bond. In order to

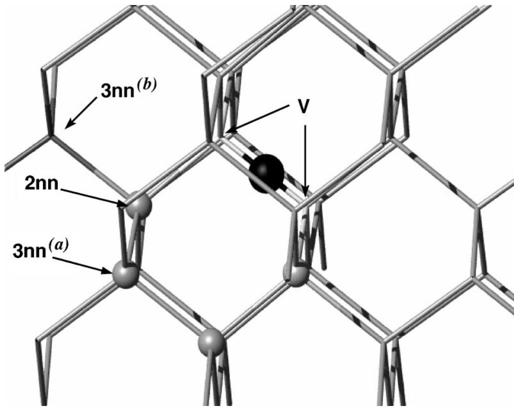

FIG. 4. Relaxed structure of the InV complex. The atoms that have undergone sizable relaxations from the initial structure are shown with spheres over the host silicon lattice (sticks). The In atom is plotted in black with larger atomic radius with respect to its nn silicon atoms. The arrows indicate the two sites over which the Si vacancy is splitted (V) and the 2nn and 3nn sites.

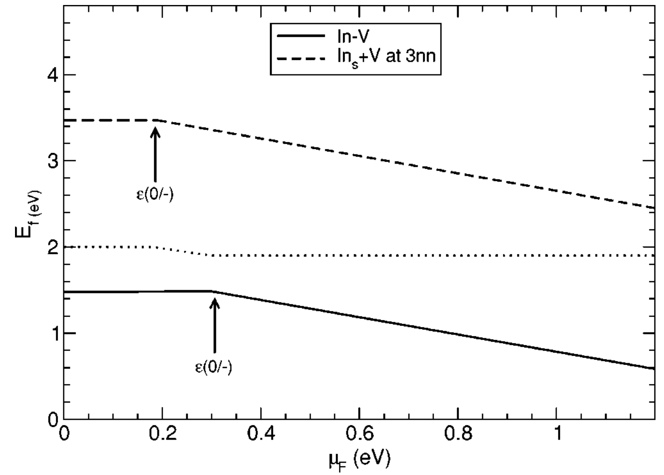

FIG. 5. Formation energy of In-vacancy defects as a function of the Fermi level μ_F. Solid lines correspond to the InV complex, dashed lines to the configuration with the Si-V placed at 3nn distance from In_s. The dotted line is the formation energy difference between the two. Electronic levels ϵ are also indicated.

complete a diffusion step, the Si_{Td} has either to diffuse away (with a new Si interstitial eventually reaching In_s from a different ⟨111⟩ direction) or to move around the substitutional In without dissociating. The energy barrier of the first process is the dissociation of the InI complex, i.e., $E_m \geqslant -E_b = 1.2$ eV, larger than the barrier of the *interstitialcy* mechanism. Instead, we perform a NEB calculation and obtain a barrier energy of $\simeq 0.6$ eV for the path connecting two InI configuration oriented along different ⟨111⟩ directions, i.e., for Si to move around the In_s atom. In the saddle-point configuration the Si interstitial sits in the 2nn-Td site of the In_s.

Thus, the two interstitial-mediated diffusion mechanisms have similar activation energy, $E_{act} = E_f + E_m \simeq 3.2$ eV. We mention also that we do not find that the diffusion mechanism depends on the charge state of the defect. Since the formation energy differences between all In-interstitial configurations are quite large, there is no crossing of $E_f(\text{In-}I^q;\mu_F)$ values when the Fermi level μ_F goes from the top of the valence band up to E_g (see Fig. 3). Thus, the energy difference between stable and metastable configurations (and consequently the migration energy) is roughly the same for any value of μ_F.

D. In-vacancy complex

The relaxed geometry of the indium-vacancy complex (InV in the following) is plotted in Fig. 4. Starting from the ideal configuration with In_s and SiV in nn positions (and checking against possible artificial symmetry-induced biases), we find that the defect undergoes large atomic relaxations that shift the In atom into a bond-center position between two empty lattice sites.

The formation energy, calculated from Eq. (1), is $E_f(\text{InV}) = 1.48$ eV. We consider the reaction $In_s^- + V^+ \rightarrow InV^0$ and calculate the defect binding energy from formation energy differences, obtaining $E_b(\text{InV}) = -2.4$ eV. This value is larger than that found for other dopant-V complexes such as P-V, As-V ($E_b \simeq -1.1/-1.6$ eV).[21] Moreover, relaxed geometries of P and As complex with Si-V do not show the substantial shift of the dopant atom towards the BC site, as in the InV geometry.[22] This suggests a strong bonding character of the InV complex that, on the basis of strain relief arguments, might be suggested as typical of dopant with larger atomic radius. Kaukonen *et al.*[23] found indeed, for instance, similar atomic relaxations for the Sn-V defect. However, as regards the complexes formed with the vacancy by the *p*-type dopants other than In (i.e., B, Al, Ga), only Al relaxes towards the BC site,[22,24] indicating that the dopant-V relaxed geometry cannot be easily predicted on the basis of a general trend.

From the formation energy values of neutral and charged InV, shown in Fig. 5 as a function of the Fermi energy, we calculate the acceptor level $\epsilon(0/-)[\text{InV}] = 0.3$ eV. The calculated $\epsilon(+/0)[\text{InV}]$ lies below the valence-band maximum. As regards the relaxed geometries of charged complexes, we find the same relaxations as for the neutral InV, i.e., In sits always in the BC position between two empty sites.

We further investigate the interactions between In and Si-V, calculating how the formation energy varies when the Si-V is placed at second- and third-nearest-neighbor distance (2nn and 3nn hereafter) from In_s.

A Si-V in a site second neighbor to In_s is unstable: the Si atom first neighbor to In_s and to the vacancy moves into the vacant site without any energy barrier, and the system reverts spontaneously into the In-divacancy complex discussed previously (Fig. 4). This relaxation indicates a monotonic increase of the energy potential when Si-V moves away from In, up to 2nn distance.

Moving further along possible dissociation paths of the InV complex, two 3nn sites can be chosen, as indicated in Fig. 4: position (a) belongs to a hexagonal ring, while (b) lies along the ⟨110⟩ chain. Placing a Si-V in positions (a) and (b) gives rise to stable structures, with still negative binding energies $E_b(3\text{nn})^{(a)} = -0.3$ eV, $E_b(3\text{nn})^{(b)} = -0.62$ eV.

On the basis of our *ab initio* calculations, we are thus able to figure out the potential energy describing the interactions between a substitutional In and a Si-V as a function of the distance d between the two. We summarize it noticing two anomalous features with respect to other dopant-V complexes energetics: the minimum of the binding energy being located at $d=d_{Si}/2$ instead of $d=d_{Si}$, and the negative slope of the binding energy at d equal to the 2nn distance, where no local minimum is detected.

We estimate the activation energy for V-mediated In diffusion on the basis of our energetics. The negative value of $E_b(3\mathrm{nn})$ indicates that the range of the interactions between In and Si-V extends beyond the third nn distance, and suggests a pair mechanism for V-mediated In diffusion.[22] The first step of any V-mediated diffusion mechanism starts with the exchange of atomic positions between In and Si-V. Then, the simplest pair-diffusion mechanism requires that the Si-V moves away to the 2nn and $3\mathrm{nn}^{(a)}$ sites and returns close to the same In atom through jumps over different 2nn and 1nn sites on the hexagonal ring.[25] The overall energy barrier for a diffusion step is thus given by the sum of the energy difference ΔE between the InV and the $3\mathrm{nn}^{(a)}$ configuration and the barrier for the 3nn $\rightarrow$ 2nn jump of the vacancy. Assuming with reasonable confidence that the barrier energy for the 3nn $\rightarrow$ 2nn jump is equal to the vacancy migration energy [$E_m(\text{Si-V})=0.2$ eV, Ref. 26], it is possible to give an estimation of the activation energy for the V-mediated pair diffusion. We plot the energy difference ΔE in Fig. 5 as a function of the Fermi energy, and note that it is roughly constant, increasing by 0.2 eV in p-type doping conditions with respect to the $\Delta E=1.9$ eV value of the intrinsic regime. Thus, $E_m=\Delta E+E_m(\text{Si-}V)=2.1$ eV and the associated activation energy is $E_{act}=3.6$ eV.

This mechanism is opposed to the simple vacancy diffusion one, where, after the two defects have exchanged positions, the In-V complex does dissociate and the Si-V migrates away, eventually finding a different dopant atom to be kicked out. The migration energy would then be the binding energy of InV, i.e., $E_m=2.2$ eV and thus $E_{act}=3.7$ eV, slightly larger than the activation energy for the pair mechanism described above.

III. DIFFUSION MODEL

The results of the *ab initio* calculations have been used in a continuum code capable of simulating the evolution of as-implanted dopant profiles on the basis of diffusion equations. A software[27] allows the integration of user supplied diffusion model in the general framework of a process simulator. We use a modeling approach that has been introduced to simulate dopant diffusion in silicon,[28,29] in which the coupling between silicon defects and any general impurities drives the impurity diffusion through the formation of mobile defect-impurity pairs. We report here a brief derivation of the relevant formula, in order to make clear how we relate the parameters of the model to the *ab initio* energetics discussed in previous sections.

At high temperature we can assume with a good approximation that all the impurity atoms under the solid solubility threshold are ionized. Therefore, we should deal with the evolution equation for the ionized impurity density field $C_{\mathrm{In}^-}\simeq C_{\mathrm{In}}$, which is

$$\dot{C}_{\mathrm{In}^-}=-R_{\mathrm{InI}^0}-R_{\mathrm{InV}^0}.$$

Here, $\dot{C}=\partial C/\partial t$ while the reaction terms $R_{\mathrm{In}X^0}$ ($X=$I,V) rule the defect-impurity coupling in the neutral channel[29] and are given by

$$R_{\mathrm{In}X^0}=K^{+}_{X^+}[C_{\mathrm{In}^-}C_{X^+}-K_{\mathrm{In}X^0}C_{\mathrm{In}X^0}], \tag{4}$$

where $K^{+}_{X^+}$ is the formation rate parameter, while C_{In^-}, C_{X^+}, $C_{\mathrm{In}X^0}$ are the density fields of the different defects, the charged In_s^- and X^+, and the pair InX in the neutral state. $K_{\mathrm{In}X^0}$ is the binding parameter, which depends on the coupling energy gain in the $\mathrm{In}^-+X^+\rightarrow \mathrm{In}X^0$ reaction. The *ab initio* binding energies $E_b(\mathrm{In}X^0)$ discussed in previous sections enter, thus, in the definition of $K_{\mathrm{In}X^0}$ through an Arrhenius-type expression, together with an entropy term $S_{\mathrm{In}X^0}$:

$$K_{\mathrm{In}X^0}=\rho_{\mathrm{Si}}\exp(-S_{\mathrm{In}X^0}/k_B)\exp[E_b(\mathrm{In}X^0)/k_BT].$$

As regards the equations that rule the diffusion of the InX pair, we first derive the expressions that relate the density of the q-charged complexes, $C_{\mathrm{In}X^q}$, to the one of the neutral pairs, $C_{\mathrm{In}X^0}$. Assuming that the electron-type reactions are much faster than the chemical ones, we can write the following expression for $C_{\mathrm{In}X^q}$:

$$C_{\mathrm{In}X^q}=[K^{e}_{\mathrm{In}X^q}]^{-1}\left(\frac{p}{n_i}\right)^{q}C_{\mathrm{In}X^0}, \tag{5}$$

where p and n_i are the hole and intrinsic charge density, respectively. In the above expression, $K^{e}_{\mathrm{In}X^q}$ is the ionization parameter, which is related to the difference between formation energies of the charged and neutral pair, calculated at midgap:

$$K^{e}_{\mathrm{In}X^q}\simeq\exp\left(\frac{E_f(\mathrm{In}X^q;E_g/2)-E_f(\mathrm{In}X^0)}{k_BT}\right).$$

If we define the total pair density as $C_{\mathrm{In}X}=\Sigma_q C_{\mathrm{In}X^q}$, Eq. (5) allows us to write

$$C_{\mathrm{In}X^0}=\frac{C_{\mathrm{In}X}}{\sum_q [K^{e}_{\mathrm{In}X^q}]^{-1}\left(\frac{p}{n_i}\right)^{q}}.$$

We can express C_{X^+} in terms of the total defect density C_X, in a similar way to Eq. (5):

$$C_{X^+}=\frac{C^{\text{int-}eq}_{X^+}}{C^{*}_{X}}\frac{p}{n_i}C_X, \tag{6}$$

where C^{*}_{X} and $C^{\text{int-}eq}_{X^+}$ are the equilibrium densities of the X defects (in neutral and + positive-charged states), in intrinsic conditions.

Finally, if the pair diffusivity $D_{\mathrm{In}X}$ is weakly dependent on the charge state (as the *ab initio* results suggest, see previous sections), we have the following diffusion equation for $C_{\mathrm{In}X}$:

$$\dot{C}_{\mathrm{In}X}=\sum_q \dot{C}_{\mathrm{In}X^q}=\nabla\left[D_{\mathrm{In}X}\left(\frac{p}{n_i}\right)^{-1}\nabla\left(\frac{p}{n_i}C_{\mathrm{In}X}\right)\right]+R_{\mathrm{In}X^0}.$$

From Eqs. (4)–(6) we can express the rate $R_{\mathrm{In}X^0}$ as

$$R_{\mathrm{In}X^0}=K_{\mathrm{eff}}^{+}[C_{\mathrm{In}^-}C_X-K_{\mathrm{In}X}(p)C_{\mathrm{In}X}],$$

where we define a Fermi-level-dependent binding parameter $K_{\mathrm{In}X}(p)$, equal to

$$[K_{\mathrm{In}X}(p)]^{-1}=\frac{C_{X^+}^{\text{int-}eq}}{C_X^*}[K_{\mathrm{In}X^0}]^{-1}\sum_q\left(\frac{p}{n_i}\right)^{q+1}[K_{\mathrm{In}X^q}^{e}]^{-1}.$$

Moreover, we can reliably approximate the rate parameter as $K_{\mathrm{eff}}^{+}=4\pi a_{\mathrm{Si}}D_X$, where a_{Si} is silicon lattice spacing and D_X is the native defect diffusivity.

Finally, in equilibrium conditions, we can derive the total impurity diffusivity due to the X defect ($D_{\mathrm{In},X}$ in the following) from the above equations,[29] and obtain the following Fermi-level-dependent expression:

$$D_{\mathrm{In},X}(p)=D_{\mathrm{In},X}^{0}+D_{\mathrm{In},X}^{+}\left(\frac{p}{n_i}\right)+D_{\mathrm{In},X}^{++}\left(\frac{p}{n_i}\right)^2, \tag{7}$$

where

$$D_{\mathrm{In},X}^{0}=[K_{\mathrm{In}X^0}]^{-1}[K_{\mathrm{In}X^-}^{e}]^{-1}C_{X^+}^{\text{int-}eq}D_{\mathrm{In}X},$$

$$D_{\mathrm{In},X}^{+}=[K_{\mathrm{In}X^0}]^{-1}C_{X^+}^{\text{int-}eq}D_{\mathrm{In}X},$$

$$D_{\mathrm{In},X}^{++}=[K_{\mathrm{In}X^0}]^{-1}[K_{\mathrm{In}X^+}^{e}]^{-1}C_{X^+}^{\text{int-}eq}D_{\mathrm{In}X}.$$

The experimental values of In equilibrium diffusion in intrinsic conditions, $D_{\mathrm{In}}^*=\Sigma_X D_{\mathrm{In},X}(n_i)$, as a function of the temperature can be fitted by an Arrhenius type expression $D_{\mathrm{In}}^*=4.04\exp(-3.701/k_BT)$.[30] As for the total interstitial contribution to the diffusivity, the experimental value is set at $f_{\mathrm{I}}=D_{\mathrm{In,I}}(n_i)/D_{\mathrm{In}}^*=0.8$.[1] We use the experimental value of D_{In}^* and f_{I} in order to fix the factors related to the entropy contributions in the diffusivity expression, while the parameters related to the intrinsic defects are taken from literature.[18,26] We note that, according to our *ab initio* results, the main contributions to charged D_{In}^* come from the neutral and positively charged InI pairs and from the negatively charged InV pairs.

We apply this diffusion model, based on our *ab initio* results, to experimental data on In diffusion in nonequilibrium conditions. In Fig. 6 we show the experimental chemical profile obtained by means of SIMS of implanted indium at 40 keV energy with a dose of 5×10^{12} ions/cm^{-2}, and further annealed at $T=800\,^\circ$C for different times, $t=20$ s [Fig. 6(a)], $t=5$ min [Fig. 6(b)] and $t=15$ min [Fig. 6(c)]. We also show the simulated profiles obtained for these process parameters (temperatures and annealing times) from the equations above, using as initial profiles the as-implanted SIMS In profiles and a residual I profile which is two times the implanted In profile.[31] Surface recombination for interstitials has been considered in the simulations as ruled by the equation

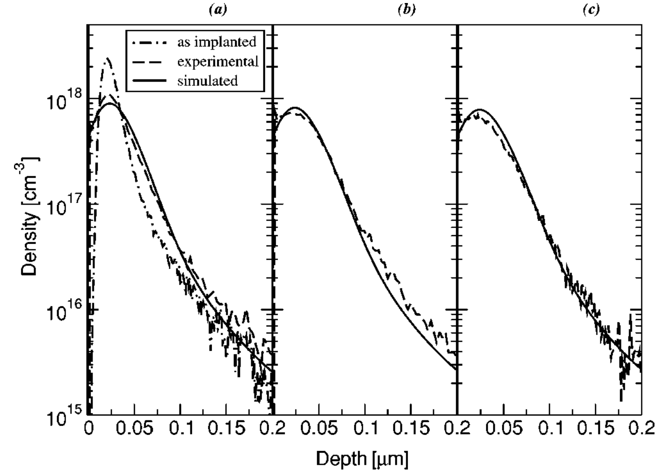

FIG. 6. SIMS In profiles (dashed lines) and simulated In profiles (solid lines) obtained after thermal annealing at temperature $T=800\,^\circ$C (implanted dose 5×10^{12} cm^{-2} ion energy 40 keV, CZ substrates) at different times (a) $t=20$ s, (b) $t=5$ min, (c) $t=15$ min. In the left graph the as-implanted profile is also shown (dots-dashed line).

$$D_{\mathrm{I}}\nabla C_{\mathrm{I}}=-K_{\mathrm{surf}}(C_{\mathrm{I}}-C_{\mathrm{I}}^*), \tag{8}$$

where $K_{\mathrm{surf}}=1.1\times10^{-3}$ cm/s can be considered as the only fitting parameter.

In the experimental conditions that we are considering, the impurity evolution occurs in a nonequilibrium transient regime and strongly depends on the concurrent defect evolution and on the defect-impurity interaction. In particular, the apparent enhanced diffusion after the 15-min thermal process is $\simeq200$ times larger than the equilibrium diffusivity D_{In}^*.[5] Therefore, in order to describe reliably the profile evolution at different time intervals, an accurate estimate of the parameters describing the defect-impurity coupling is needed. Therefore, we use the parameters ruling the energetics of the diffusion mechanisms emerging from our *ab initio* calculations. From the comparison shown in Fig. 6 we can observe a noteworthy agreement between the experimental data and the results of the modeling, demonstrating the accuracy of our *ab initio* results and the validity of the present combined approach to model In diffusion.[32]

IV. CONCLUSIONS

We have performed first-principles total-energy calculations within the density-functional theory for different In-related defects in silicon, investigating the isolated substitutional In atom as well as the In-interstitial and In-vacancy complexes, in different charge states. We find that the most stable In-interstitial defect is a pair formed by a substitutional In and a nearby tetrahedral Si interstitial. The energy difference between other metastable In-interstitial structures is $\geqslant0.5$ eV for any position of the Fermi energy. The structure of the In-vacancy complex shows large relaxations from

the ideal geometry, since the In atom occupies a bond-center position between two empty silicon lattice sites.

We have investigated the I- and the V-mediated diffusion mechanisms, identifying the two diffusion paths and finding activation energies in the same energy range ($E_{act}^{\mathrm{I}} \simeq 3.2$ eV, $E_{act}^{\mathrm{V}} \simeq 3.6$ eV). The separate contributions of migration and formation energy are however different in the two cases, with the migration energy for the interstitialcy path smaller than the barrier for the InV to diffuse.

The implementation of the *ab initio* results into a continuum model based on coupled diffusion equations for the density fields of all In-related defects ($\mathrm{In_s}$, InI, and InV) is shown to be very effective in obtaining an accurate modeling of the experimental profiles.

Finally, we notice that this approach corresponds to a general need felt in the microelectronic simulation community. Simulation tools can only be useful and predictive when based on a small number of physically meaningful parameters whose value can be predicted (or measured) reliably. In this respect, *ab initio* calculations can and do play a major role, not fully appreciated so far.

ACKNOWLEDGMENTS

We acknowledge computational support from the CINECA computing center in Bologna, under the CINECA-CNR agreement. This work was supported by the European Project "*Front-End Models for Silicon Future Technology*" (FRENDTECH), Contract No. IST-2000-30129. P.A. thanks V. Fiorentini for useful discussions.

---

*Electronic address: paola.alippi@imm.cnr.it

[1] I.C. Kizilyalli, T.L. Rich, F.A. Stevie, and C.S. Rafferty, J. Appl. Phys. **80**, 4944 (1996).
[2] P.B. Griffin, M. Cao, P. Vande Voorde, Y.-L. Chang, and W.G. Greene, Appl. Phys. Lett. **73**, 2986 (1998).
[3] H. Boudinov, J.P. de Souza, and C.K. Saul, J. Appl. Phys. **86**, 5909 (1999).
[4] S. Solmi, A. Parisini, M. Bersani, D. Giubertoni, V. Soncini, G. Carnevale, A. Benvenuti, and A. Marmiroli, J. Appl. Phys. **92**, 1361 (2002).
[5] S. Scalese, M. Italia, A. La Magna, G. Mannino, V. Privitera, M. Bersani, D. Giubertoni, M. Barozzi, S. Solmi, and P. Pichler, J. Appl. Phys. **93**, 9773 (2003).
[6] R. Baron, J.P. Baukus, S.D. Allen, T.C. McGill, M.H. Young, H. Kimura, H.V. Winston, and O.J. Marsh, Appl. Phys. Lett. **34**, 257 (1979).
[7] D.A. Antoniadis and I. Moskowitz, J. Appl. Phys. **53**, 9214 (1982).
[8] K. Suzuki, H. Tashiro, and T. Aoyama, Surf. Sci. Spectra **43**, 27 (1999).
[9] G. Kresse and J. Hafner, Phys. Rev. B **47**, 558 (1993); **49**, 14 251 (1994); G. Kresse and J. Furthmüller, Comput. Mater. Sci. **6**, 15 (1996); Phys. Rev. B **54**, 11 169 (1996).
[10] J.P. Perdew, *Electronic Structure of Solids'91*, edited by P. Ziesche and H. Eschrig (Akademie-Verlag, Berlin, 1991), p. 11.
[11] D. Vanderbilt, Phys. Rev. B **40**, 7892 (1990).
[12] M. Leslie and M.J. Gillan, J. Phys. C **18**, 973 (1985); G. Makov and M.C. Payne, Phys. Rev. B **51**, 4014 (1995).
[13] A. Zoroddu, F. Bernardini, P. Ruggerone, and V. Fiorentini, Phys. Rev. B **64**, 045208 (2001).
[14] C.E. Jones and G.E. Johnson, J. Appl. Phys. **52**, 5159 (1981).
[15] S.M. Sze, *Physics of Semiconductors Devices* (Wiley, New York, 1981), p. 22–27.
[16] Xuan Luo, S.B. Zhang, and Su-Huai Wei, Phys. Rev. Lett. **90**, 026103 (2003).
[17] J.E. Northrup, M.C. Schabel, C.J. Karlsson, and R.I.G. Uhrberg, Phys. Rev. B **44**, 13 799 (1991).
[18] G. Lopez and V. Fiorentini (unpublished).
[19] H. Jonsson, G. Mills, and K.W. Jacobsen, in *Classical and Quantum Dynamics in Condensed Phase Simulations*, edited by B.J. Berne, G. Ciccotti, and D.F. Coker (World Scientific, Singapore, 1998).
[20] W. Windl, M.M. Bunea, R. Stumpf, S.T. Dunham, and M.P. Masquelier, Phys. Rev. Lett. **83**, 4345 (1999); B. Sadigh, T.L. Lenosky, S.K. Theiss, M.J. Caturla, T.D. de la Rubia, and M.A. Foad, *ibid.* **83**, 4341 (1999).
[21] M. Ramamoorthy and T.P. Pantelides, Phys. Rev. Lett. **76**, 4753 (1996).
[22] J.S. Nelson, P.A. Schultz, and A.F. Wright, Appl. Phys. Lett. **73**, 247 (1998).
[23] M. Kaukonen, R. Jones, S. Oberg, and P.R. Briddon, Phys. Rev. B **64**, 245213 (2001).
[24] G. Lopez and V. Fiorentini (private communication).
[25] P.M. Fahey, P.B. Griffin, and J.D. Plummer, Rev. Mod. Phys. **61**, 289 (1989).
[26] G.D. Watkins, in *Deep Centers in Semiconductors*, 2nd ed., edited by S.T. Pantelides (Gordon and Breach, Switzerland, 1992), Chap. 3.
[27] http://www.tec.ufl.edu/flooxs: FLOOPS process simulator, ISE TCAD Release 9.0, User's Manual, ISE AG, Zurich.
[28] M. Orlowski, Appl. Phys. Lett. **53**, 1323 (1988).
[29] M.E. Law, H. Park, and P. Novell, Appl. Phys. Lett. **59**, 3488 (1991).
[30] P. Pichler (private commmunication).
[31] G. Hobler, L. Pelaz, and C.S. Rafferty, J. Electrochem. Soc. **147**, 3494 (2000).
[32] A. La Magna, S. Scalese, P. Alippi, G. Mannino, V. Privitera, M. Bersani, and C. Zechner, Appl. Phys. Lett. **83**, 1956 (2003).